

Atomistic simulation of functional organic materials: Problems and prospects

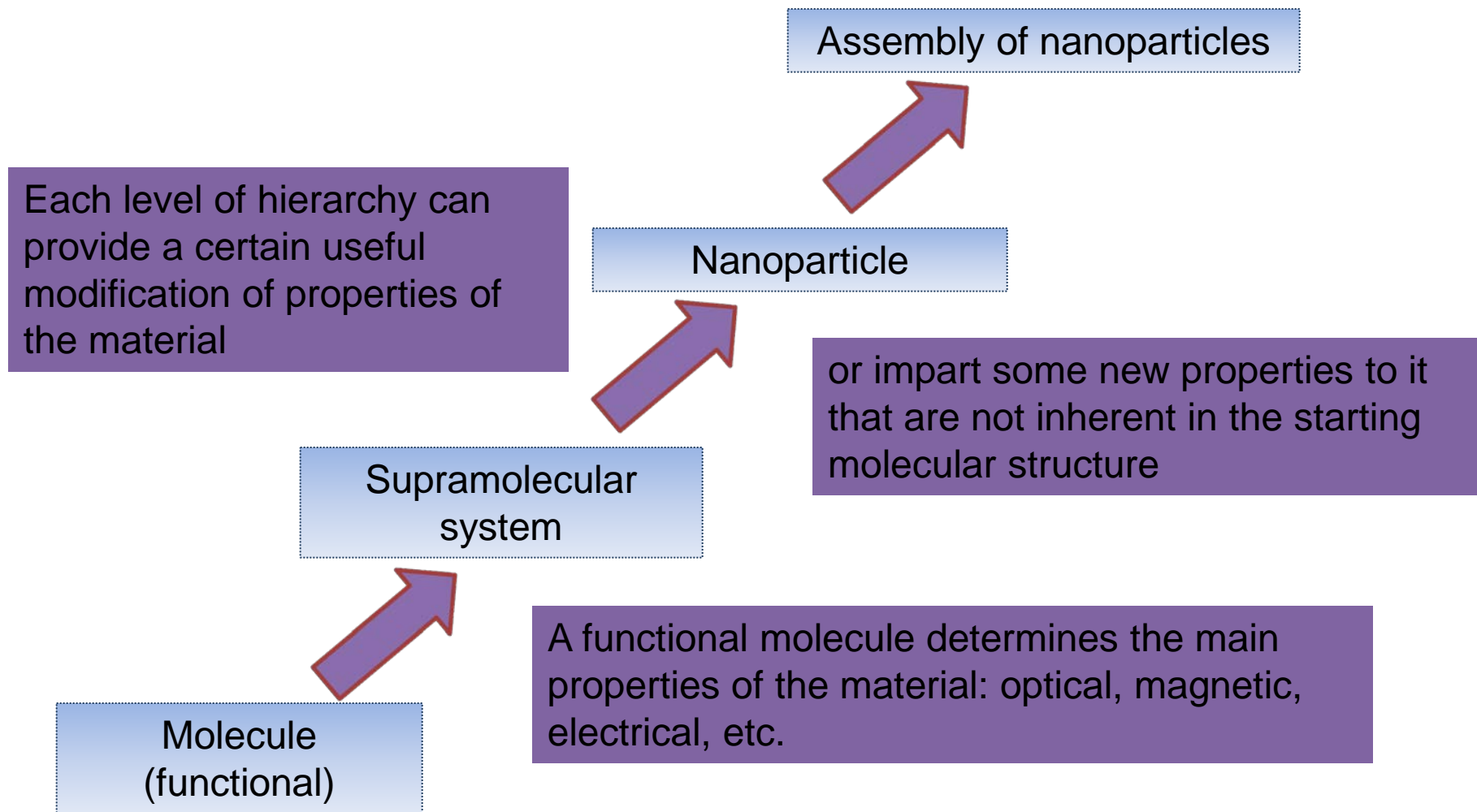


Paul Gauguin. Where Do we come from? Who are we? Where are we going?

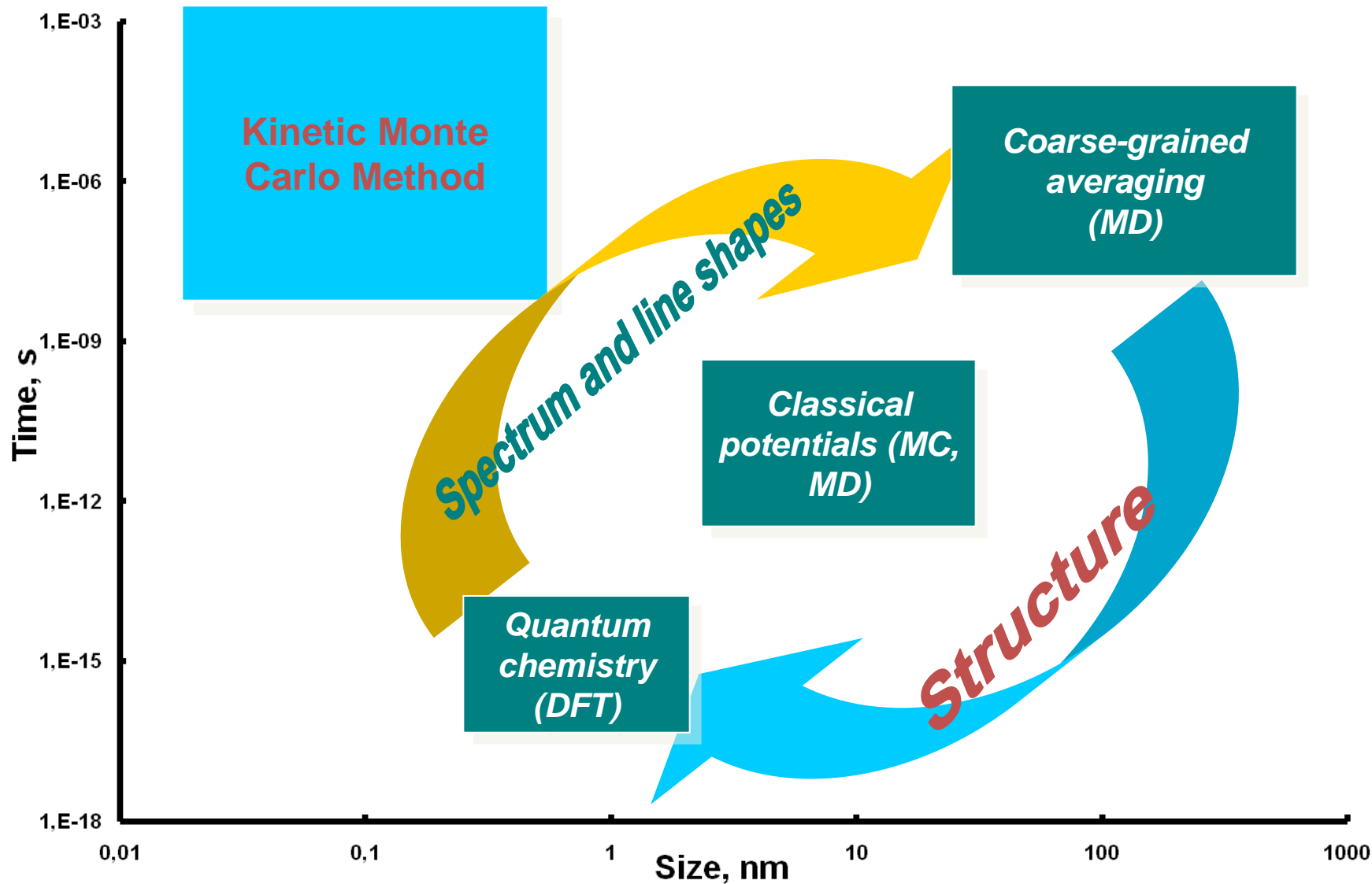
- The goal of this presentation is to show how many important properties of functional materials for sensing (optical chemical sensors) and photonics applications (organic photovoltaic and light-emitting devices) can be predicted using

Multiscale atomistic simulation

Hierarchically designed nanostructured materials

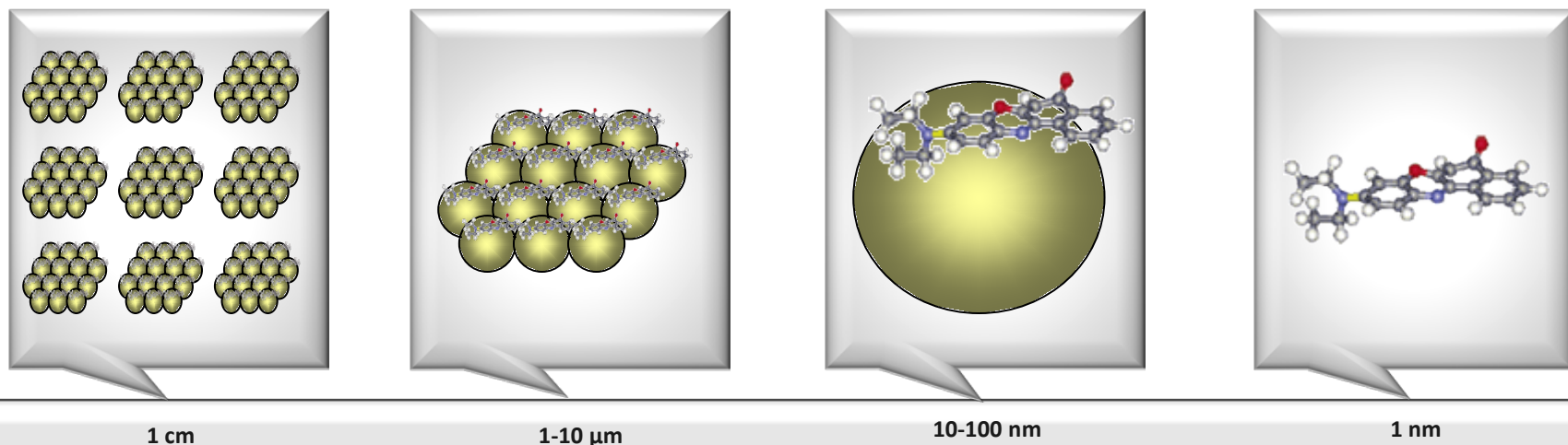


Multiscale approach in atomistic simulation of hierarchically designed nanostructured material



Part 1:
Optical Chemical Sensors

Material for optical chemical sensing as an example of hierarchically designed nanostructured material



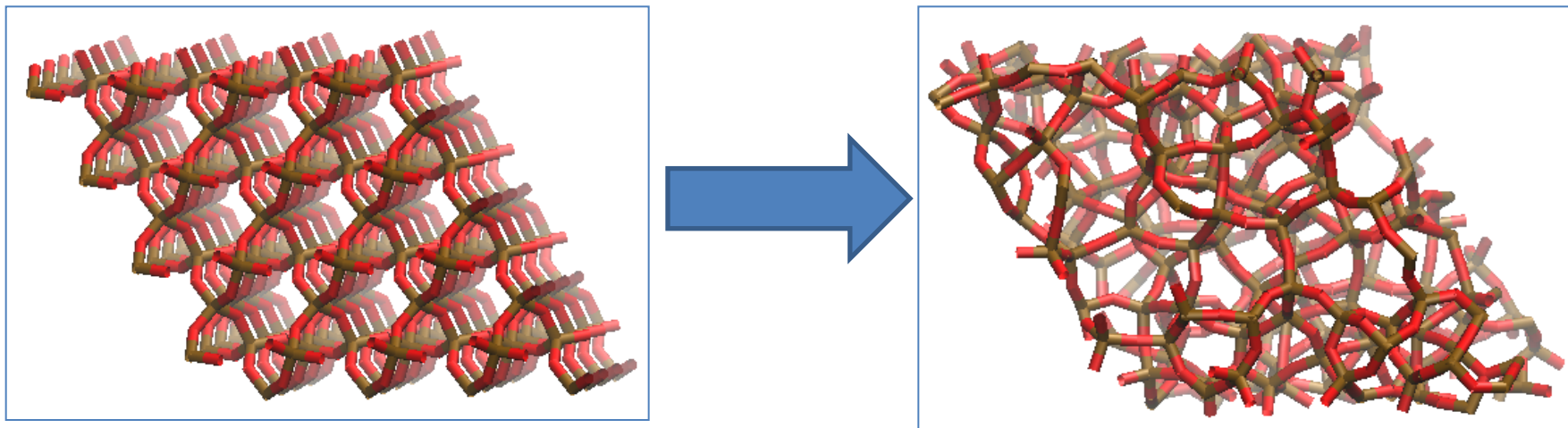
An optical chemosensor is designed for detecting various chemical compounds (analytes) in the gas phase and represents a hierarchically organized array of sensing elements constructed from various sensor materials.

An organic “indicator molecule” (IM) is responsible for the generation of an optical signal on its interaction with an analyte.

IM along with its local environment forms a “receptor center” (RC). The local environment can be organized so that the signal can be enhanced and its selectivity can be improved.

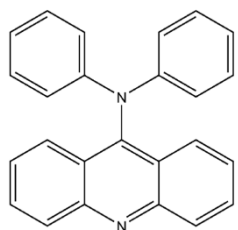
RC are arranged on the surface or in the particle bulk (nanoparticles) and the nanoparticles themselves are assembled in an organized structure (which may, for example, exhibit properties of a photonic crystal).

Modeling amorphous silica substrate

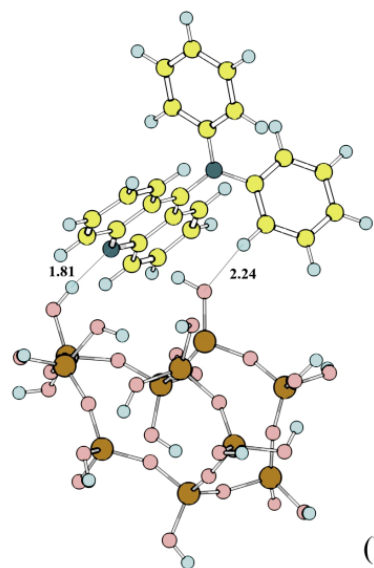


An amorphous SiO_2 structure was constructed by simulated annealing of alpha quartz using classical MD (MD-kMC program); 4x4x4 (476 atoms) T=7000 K, 50 ps; T=6500 K, 15 ps; T=6000 K, 15 ps; T=4000 K, 15 ps; T=2000 K, 15 ps; T=1000 K, 15 ps; T=300 K, 15 ps

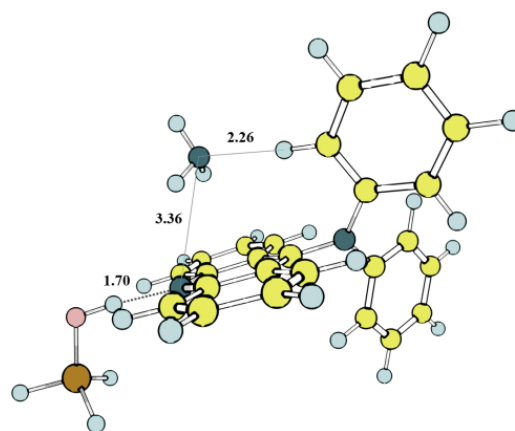
Modeling of a 9-DPAA/silica gel receptor center



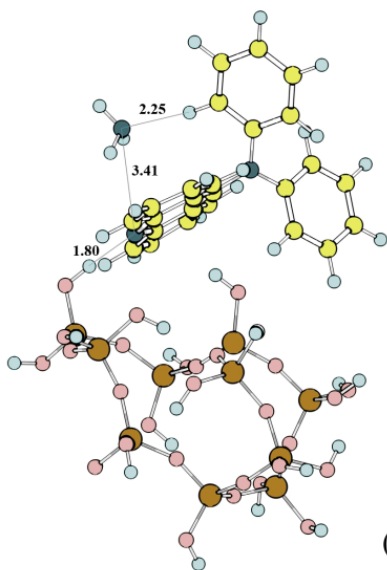
(a)



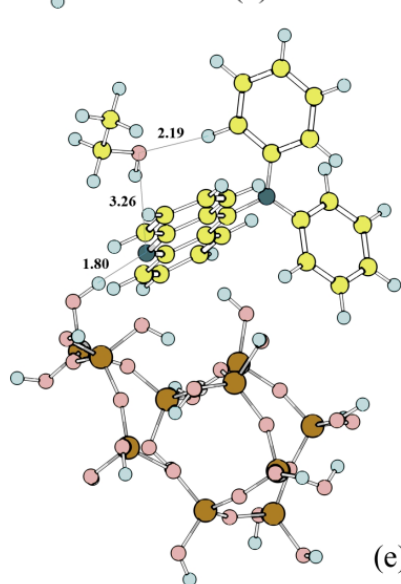
(b)



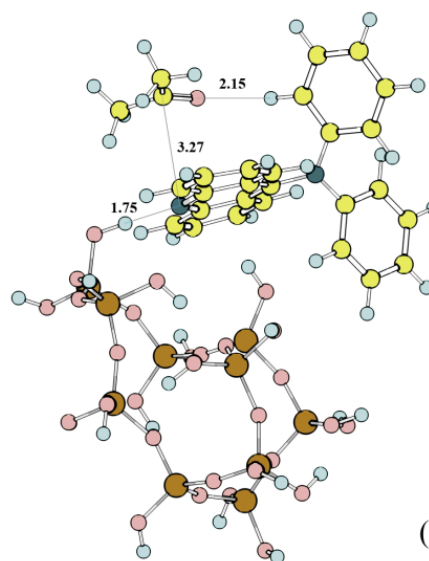
(c)



(d)



(e)



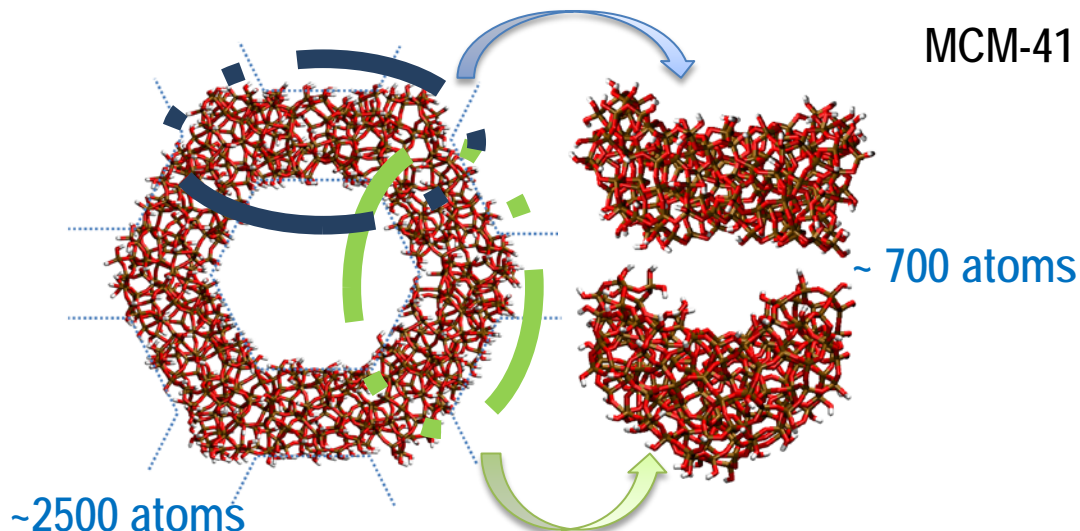
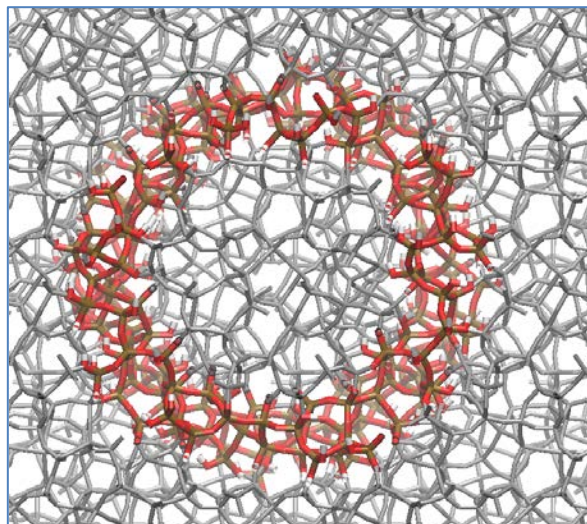
(f)

- (a) 9-DPAA
- (b) DPAA-Si10,
- (c) NH₃-DPAA-Si1,
- (d) NH₃-DPAA-Si10,
- (e) C₂H₅OH-DPAA-Si10,
- (f) (CH₃)₂CO-DPAA-Si10.

Silicon atoms are brown;
oxygen, pink; hydrogen,
blue; carbon, yellow; and
nitrogen, sea-green.

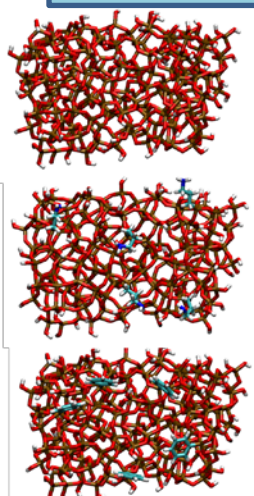
V. Chashchikhin, E. Rykova,
A. Bagaturyants, Phys.
Chem. Chem. Phys., 2011,
vol. 13, 1440–1447.

Modeling amorphous and porous (MCM-41) silica substrate

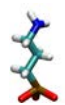


An atomistic model of the MCM-41 surface was built by cutting a hexagonal pore with a diameter of 2.5 nm out of an amorphous SiO₂ structure. The obtained pore model was cut into four 700-atomic clusters with a hydroxylation degree of 2 OH group per nm²

Surface modification



2 OH/nm²



1 Am/nm²
1 OH⁺/nm²



1 Ph/nm²
1 OH⁺/nm²

Analyte molecules



Acetone



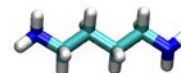
Water



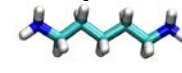
Ammonia



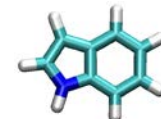
Methylamine



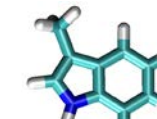
Putrescine



Cadaverine



Indole



Skatole

Modeling amorphous silica

Various products of the decomposition of amino acids and proteins (as a result of enzymatic hydrolysis due to the action of ammonifying microorganisms) adsorbed on mesoporous silica MCM-41 were investigated using multiscale simulation (QC + MD) methods.

The Gibbs free energy of formation of intermolecular complexes between these small molecules and different surfaces of mesoporous silica was calculated using a thermodynamic integration approach. The integration trajectory was obtained by molecular dynamics using the MMFF94 force field. It is found that silica surface modification with various groups affects the calculated complex formation energies.

Modeling amorphous silica substrate

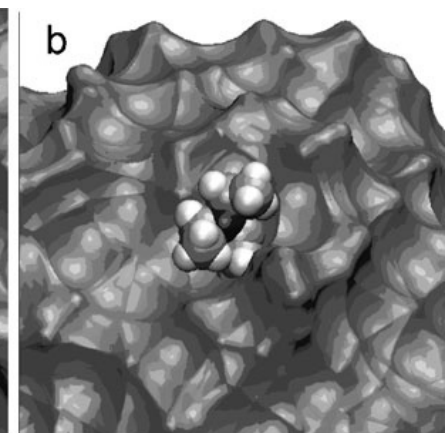
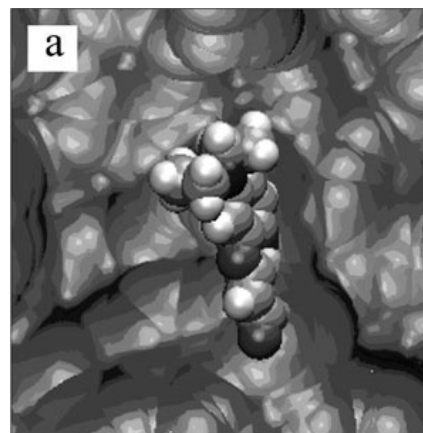
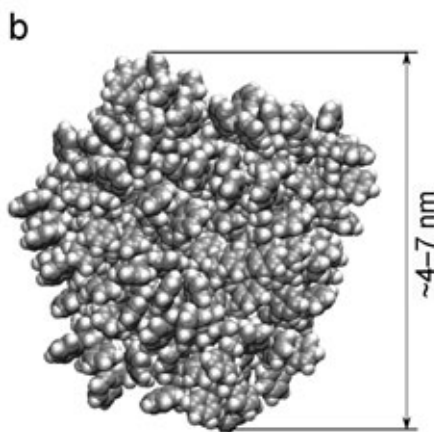
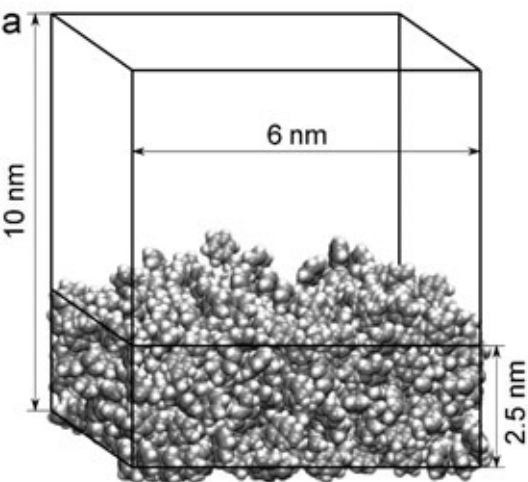
The results of free Gibbs energy calculations
(averaged over eight estimates, kcal/mol)

	acetone	ammonia	water	cadaverine	putrescine	indole	skatole	methylamine
OH	-5.2	-1.9	-2.3	-9.5	-8.8	-8.0	-7.3	-3.7
Ph	-4.3	-1.8	-2.3	-7.4	-5.7	-5.8	-6.5	-3.1
Am	-3.6	-1.3	-2.2	-6.7	-6.5	-6.3	-7.8	-2.4

The calculated free Gibbs energy for acetone (-5.2 kcal/mol) is in good agreement with the experimental value -4.5 kcal/mol. The results of this study can be used for the virtual design of optical chemical sensors for the determination of these substances in extremely low concentrations.

V. Chashchikhin, E. Rykova, A. Bagaturyants, *J. Phys. Chem. Lett.* 2013, 4, 2298–2302.

Modeling of Nile Red dye adsorption on an amorphous polystyrene surface



The structures of polystyrene used as substrate for the adsorption of the dye:

- (a) film, the integration cell is shown;
- (b) ball, the integration cell in this case has no boundaries.

A section of the solvent-accessible surface (SAS) of polystyrene with the adsorbed dye.

Acetone was a test particle, $R = 0.35$ nm:

- (a) film;
- (b) ball, a chain of 200 monomers.

V. A. Tikhomirov, A. V. Odinkov, A. A. Bagatur'yants, M.V. Alfimov, *Theor. Experim. Chemistry*, v. 46 (6), 342-349, 2011.

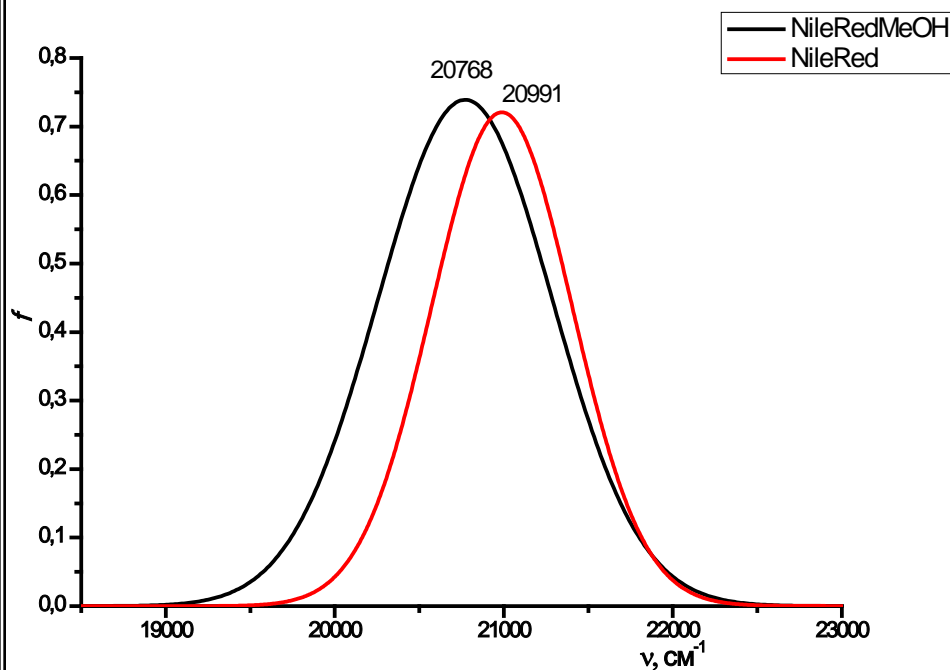
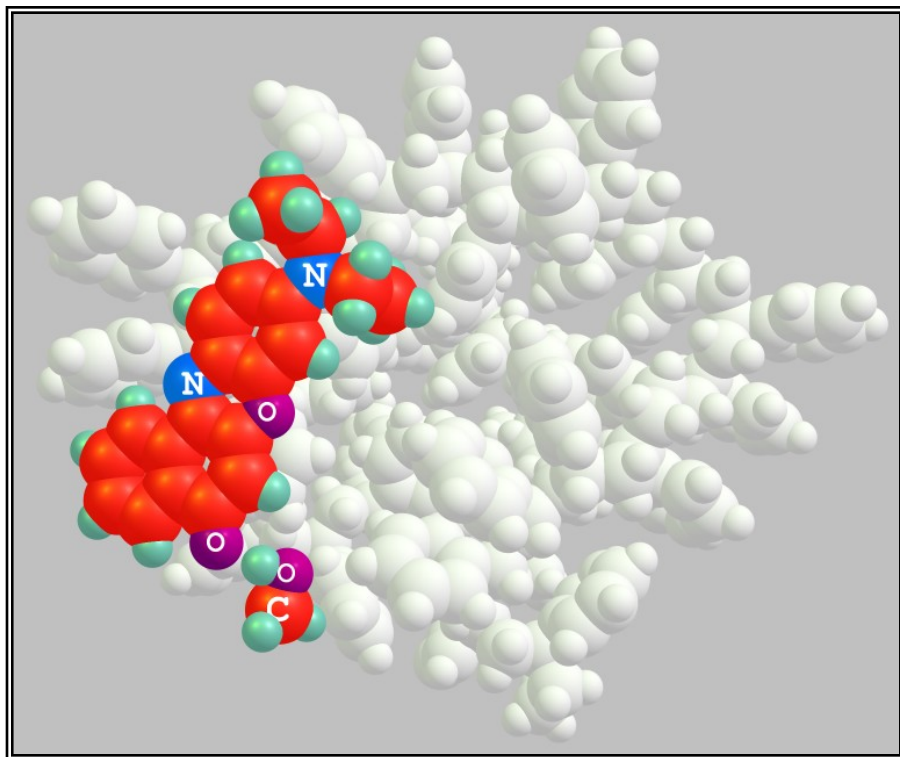
Modeling of Nile Red adsorption on an amorphous polystyrene surface



Chain of atactic polystyrene, 100 ps (500 monomer links)

Interaction of Nile Red dye on a polystyrene surface with small molecules

Search for the global minimum in the system using a genetic algorithm for the determination of the most stable configuration of a 1:1 complex between a small molecule and the Nile Red



Formation of a dye complex with methanol on a polystyrene surface, $E_b = 9.7 \text{ kcal/mol}$

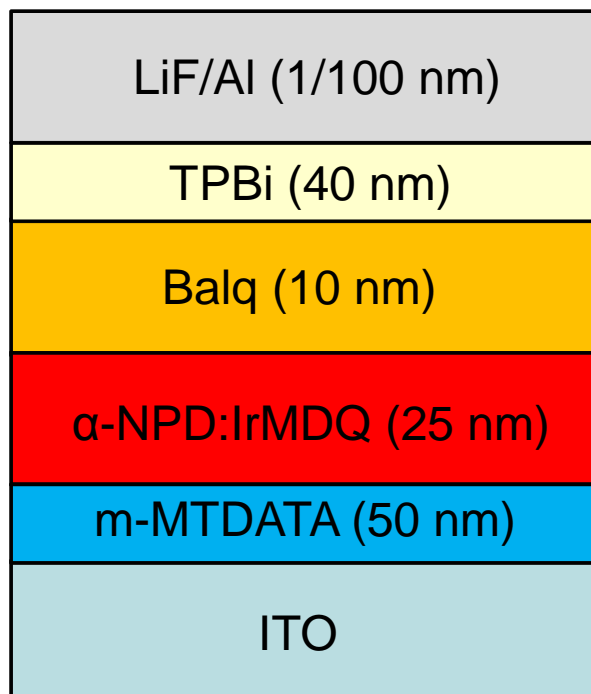
Luminescence band shift due to the formation of a dye complex with methanol $D = 223 \text{ cm}^{-1}$

CONCLUSION: A METHODOLOGY IS DEVELOPED FOR PREDICTIVE MODELING OF SILICA- AND POLYMER-BASED MATERIALS FOR OPTICAL CHEMICAL SENSORS

- ❖ **M.V. Alfimov, A.A. Bagatur'yants, A.A. Safonov, A.V. Scherbinin, K.G. Vladimirova, S.A. Belousov, M.V. Bogdanova, I.A. Valuev, A.V. Deinega, Yu.E. Lozovik, B.V. Potapkin**, Multiscale Computer Design of Photonic Crystal Based Materials for Optical Chemosensors, *Nanotechnologies in Russia*, 2010, Vol. 5, Nos. 3–4, pp. 250–258.
- ❖ **F.V. Grigor'ev, A.N. Romanov, D.N. Laikov, S.N. Zhabin, A.Yu. Golovacheva, I.V. Oferkin, A.V. Sulimov, M.V. Bazilevskii, A.A. Bagatur'yants, V.B. Sulimov, M.V. Alfimov**, Molecular Modeling Methods for Supramolecular Complexes: A Hierarchical Approach, *Nanotechnologies in Russia*, 2010, Vol. 5, Nos. 5–6, pp. 290–298.
- ❖ **A. Bagaturyants, M. Alfimov**, in *Chemical Sensors: Simulation and Modeling Vol. 4: Optical Sensors*, Ed. G. Korotcenkov, Momentum Press, 2013, pp. 1–38.

Part 2: Light-Emitting Devices

Model OLED Stacks



Working stack

TPBi = 1,3,5-Tris(1-phenyl-1H-benzimidazol-2-yl)benzene

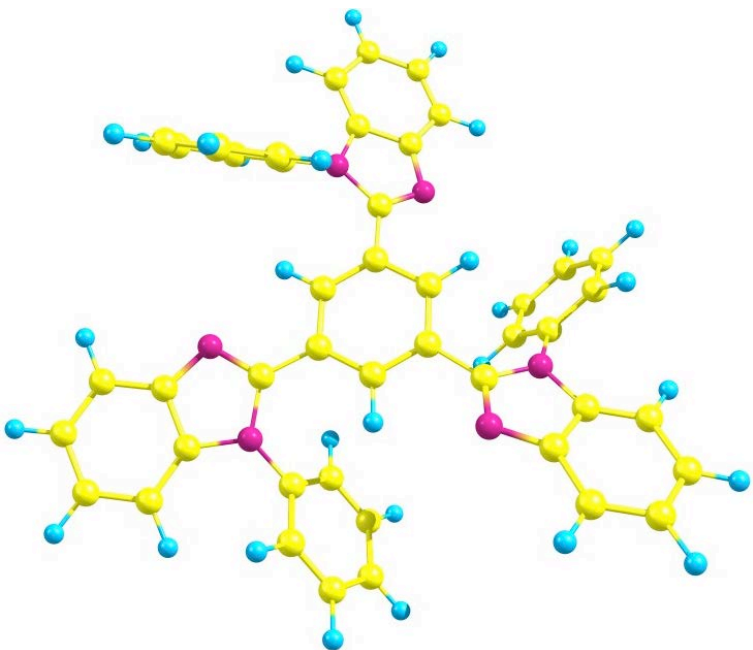
BAIq = Bis(2-methyl-8-quinolinolato-N1,O8)-(1,1'-Biphenyl-4-olato) aluminum

α -NPD = N,N'-di(naphthalen-2-yl)-N,N'-diphenyl-benzidine

IrMDQ = iridium(III)bis(2-methyldibenzo-[f,h]quinoxaline)(acetylacetonate)

m-MTDATA = 4,4',4''-Tris(N-3-methylphenyl-N-phenylamino)triphenylamine

Electron injection/hole blocking layer, 40 nm: TPBi



TPBi optimized structure

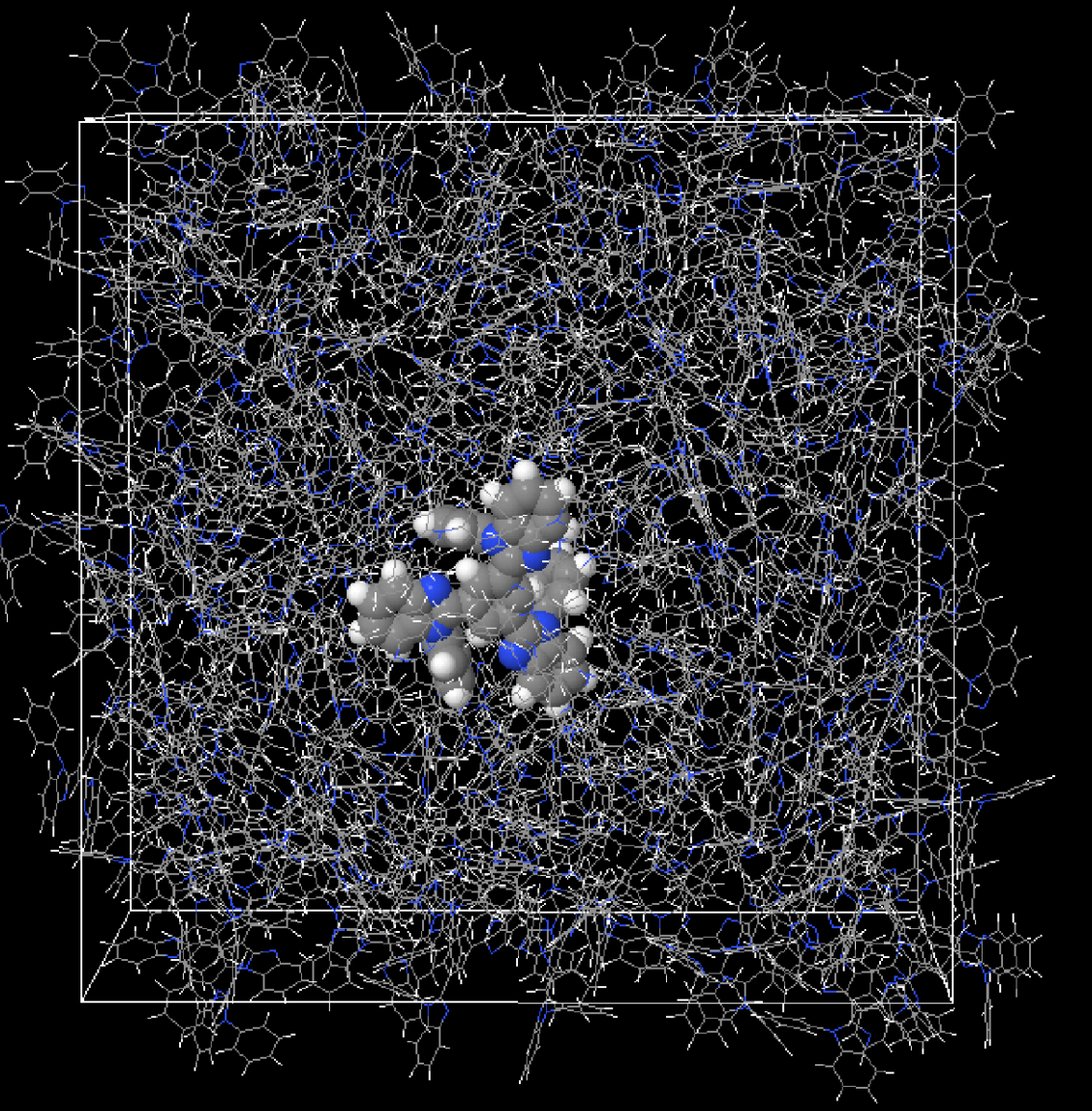
The dendritic 1,3,5-tris(*N*-phenyl-benzimidazol-2-yl)benzene (TPBi) molecule is used both as a host material and as an electron transport material (ETM) for OLEDs based on fluorescent and phosphorescent emitters. Compared to Alq₃, TPBi has a lower EA (2.7 eV) and a higher IP (6.2-6.7 eV).

Unlike Alq₃, TPBi can act as a host or ETM for blue emitters due to its higher optical band gap. Bright blue emission (11 000 cd/m²) was achieved from a phenylene vinylene oligomer emitter while using TPBi as the electron-transporting host.

Additionally, TPBi showed better hole blocking than Alq₃ due to its higher IP. Using TPBi as the ETM in an OLED based on blends of a phosphorescent Ir complex, 10.4% EQE was obtained at much lower voltages compared to those without TPBi. As a hole blocker, TPBi was shown to be more effective than bathocuproine (BCP), giving more stable OLEDs with repeatable operation. The TPBi diodes gave higher device efficiencies (55 cd/A) compared with BCP (~25 cd/A).

A.P. Kulkarni, et al., Chem. Mater., 2004, Vol. 16, № 23, p. 4556-4573.

A cell of 144 TPBi molecules

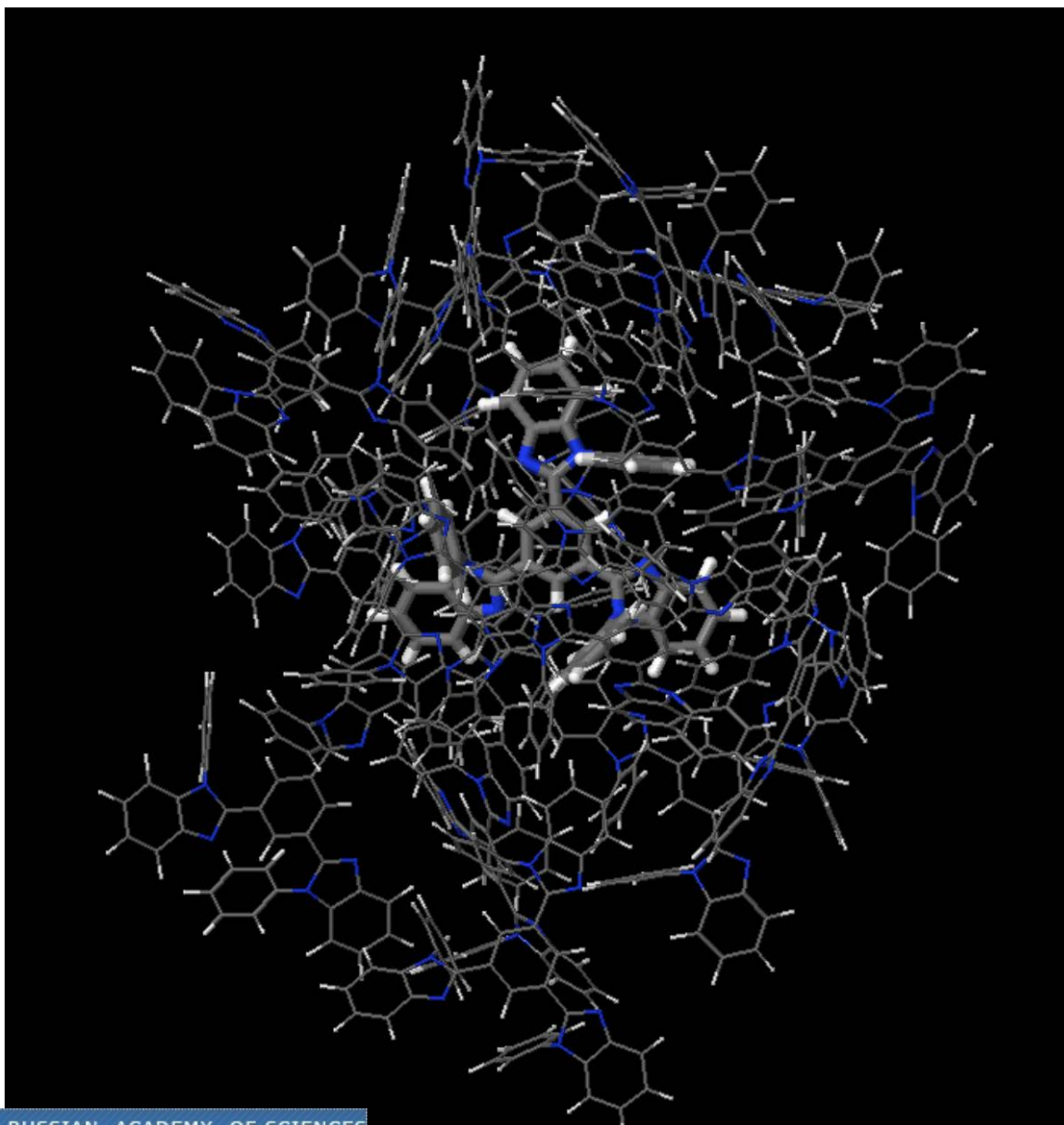


144 Molecules of TPBi were placed in a random position and orientation in a 7x7x7 nm cell (MC method).

After that an MD integration was made for 500 ps at a temperature of 900 K, each side of the cell was decreased at a constant rate until the density of the material was equal to the experimental one. Then, MD simulation was performed for 500 ps at a constant temperature of 600 K with a variable volume of the cell (NPT ensemble).

At the last stage, MD simulation was made at 298 K for 500 ps. Ten independent calculations was made using this scheme to obtain 10 cells with 1440 molecules in total.

TPBi molecule in a layer and its neighborhood



The number of molecules per unit volume: 1.04 molecules/nm³

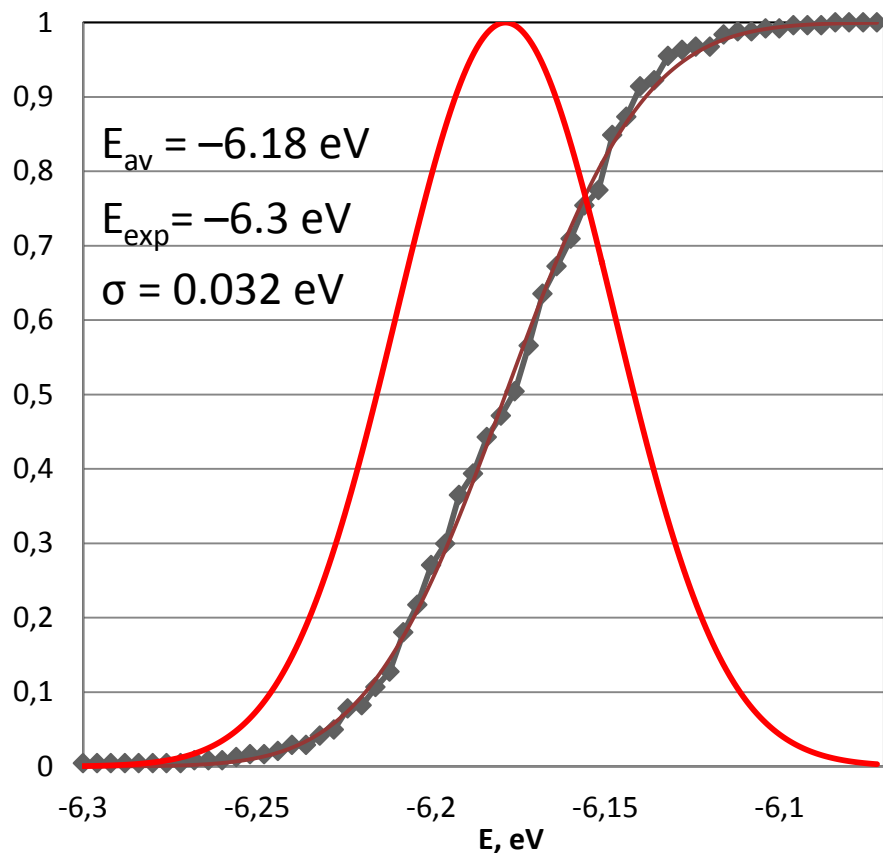
The average distance between the centers of molecules 6.1 Å

The average number of neighbors 16 ± 3 for close contacts at a distance of 5 Å

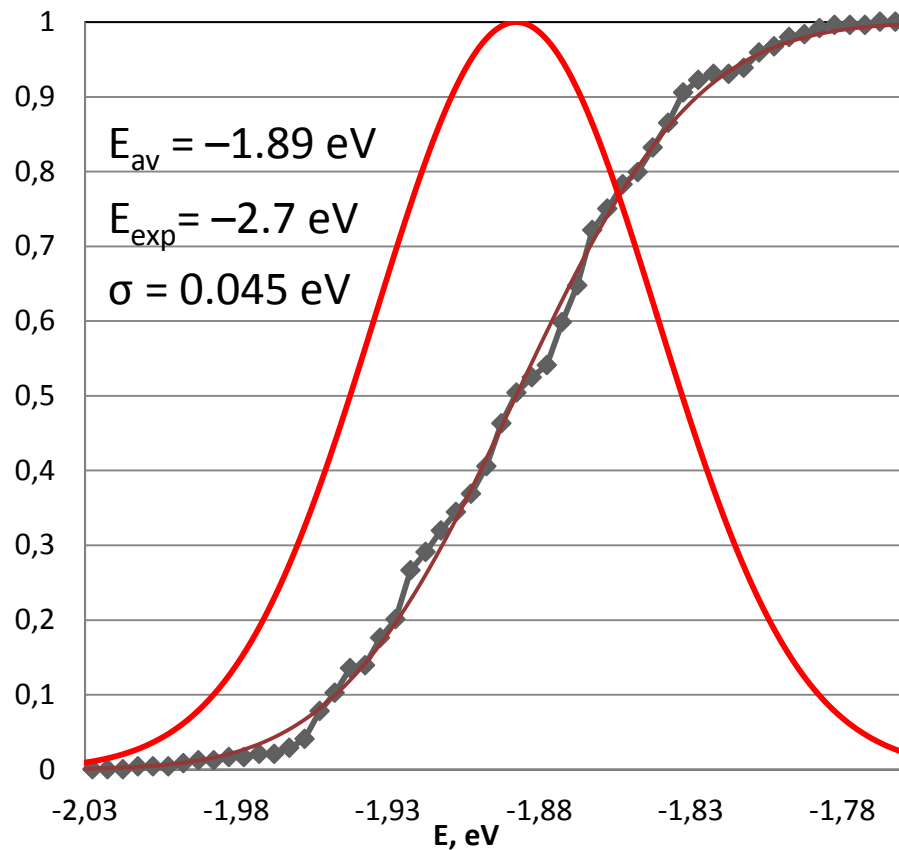
Distribution of TPBI HOMO and LUMO energies (PCM)

DFT-D, PBE0, Basis set 6-311(d,p) or cc-pVTZ, PCM: $R_{\text{SOLVENT}} = 8 \text{ \AA}$, $\epsilon = 3$, $\epsilon_{\text{inf}} = 3$, 240 molecules
Range of total energies $E_{\text{max}} - E_{\text{min}} = 1.65 \text{ eV}$ (6-311(d,p)), 1.01 eV (cc-pVTZ)

HOMO



LUMO



TPBi Reorganization energy

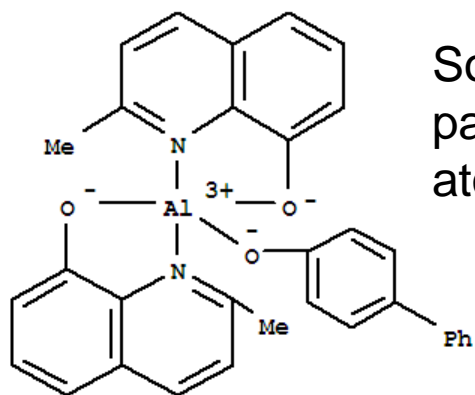
Method: DFT-D, PBE0; Basis sets: 6-311(d,p) and cc-pVTZ;

PCM: $R_{\text{SOLVENT}} = 8 \text{ \AA}$, $\epsilon = 3$, $\epsilon_{\text{inf}} = 3$

	6-311(d,p)	CCT
$\Delta E_n = E_{\text{an}}^{(n)} - E_n^{(n)}$	-1,40 eV	-1,43 eV
$\Delta E_{\text{an}} = E_{\text{an}}^{(\text{an})} - E_n^{(\text{an})}$	-1,79 eV	-1,82 eV
$E_{\text{reorg}} = \Delta E_n - \Delta E_{\text{an}}$	0,39 eV	0,39 eV

Modeling of the Balq (Bis(2-methyl-8-quinolinolato-N1,O8)-(1,1'-Biphenyl-4-olato)aluminum) layer

At the first step, we calculated the structure and electronic spectra of the BALq molecule. QC structure calculations: DFT-D, PBE functional, SVP basis set. Its chemical and optimized structures are presented below.



Some force field parameters for the Al atom are lacking.

scan parameters:

bond length Al-O₁ = R₁

bond length Al-O₂ = R₂

angle Al-O₁-C₁ = φ_1

angle Al-O₂-C₂ = φ_2

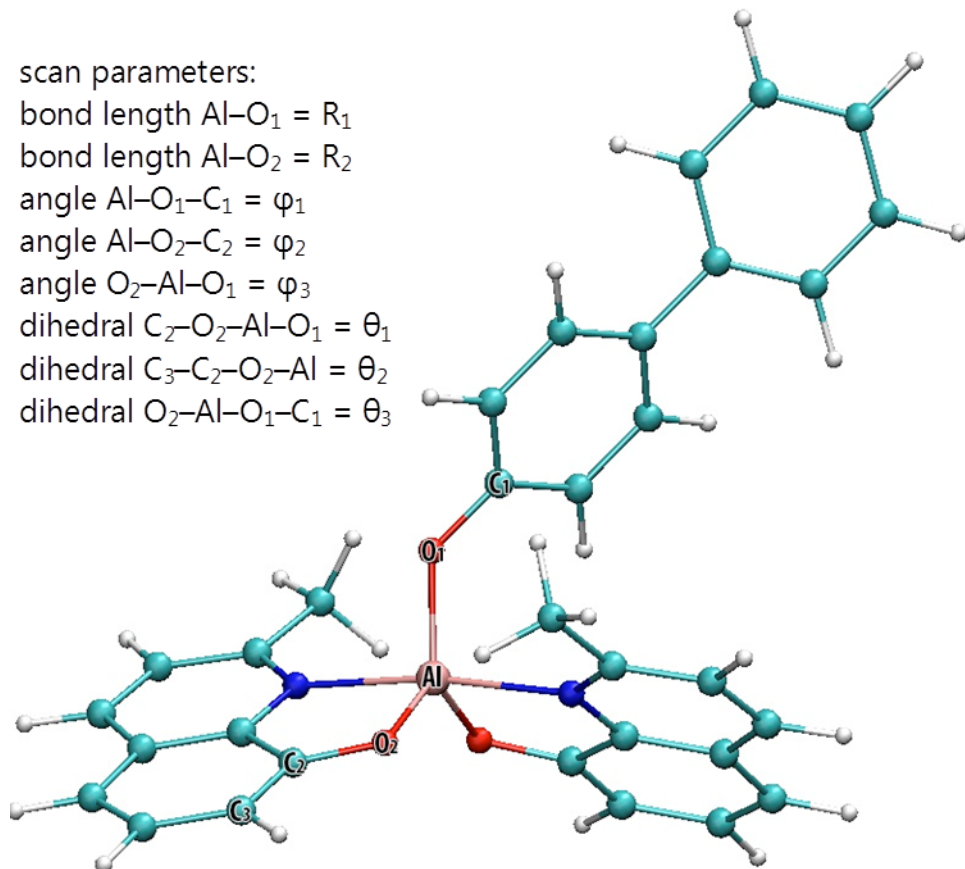
angle O₂-Al-O₁ = φ_3

dihedral C₂-O₂-Al-O₁ = θ_1

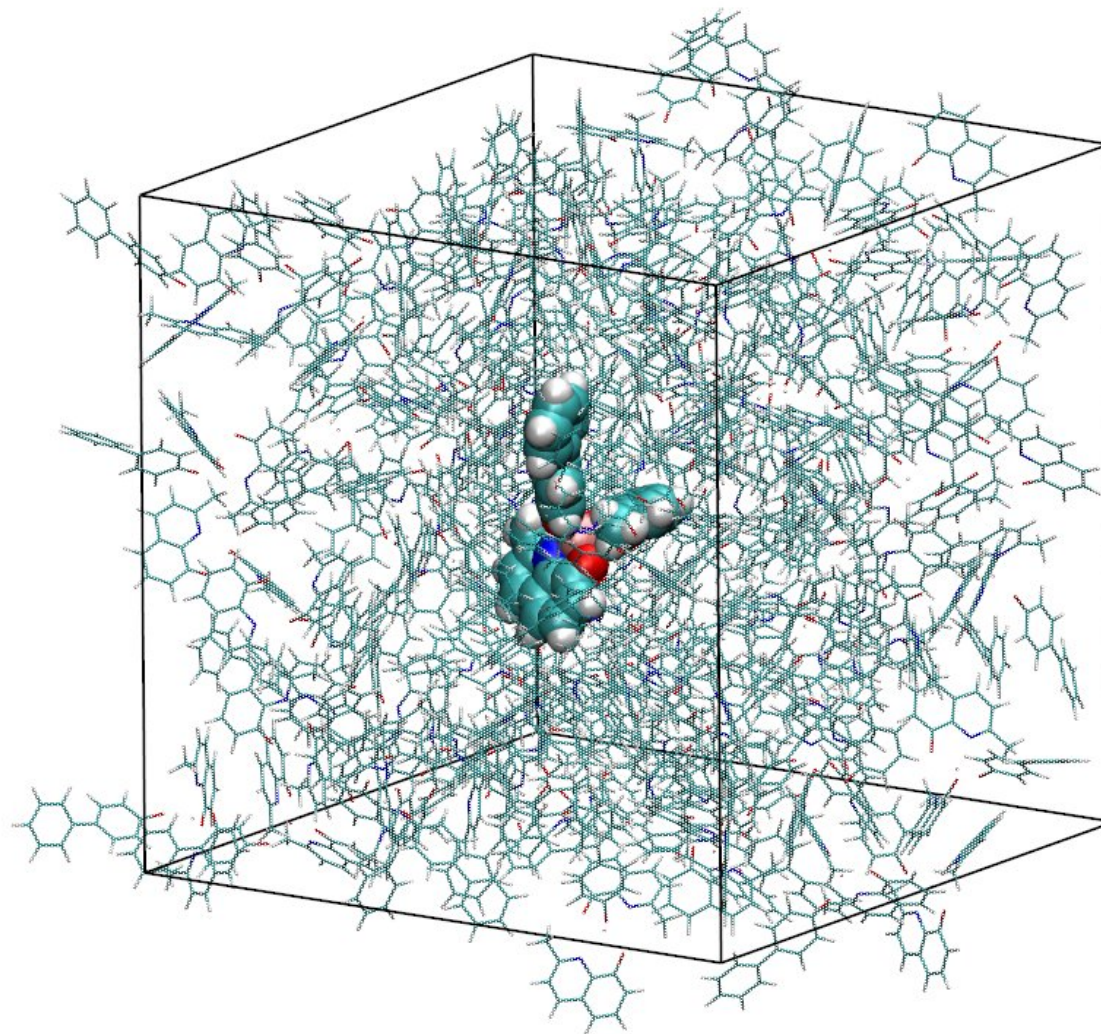
dihedral C₃-C₂-O₂-Al = θ_2

dihedral O₂-Al-O₁-C₁ = θ_3

The reorganization energy $E_r(\text{HF}) = 0.52$ eV. The most intense transition is at 387 nm

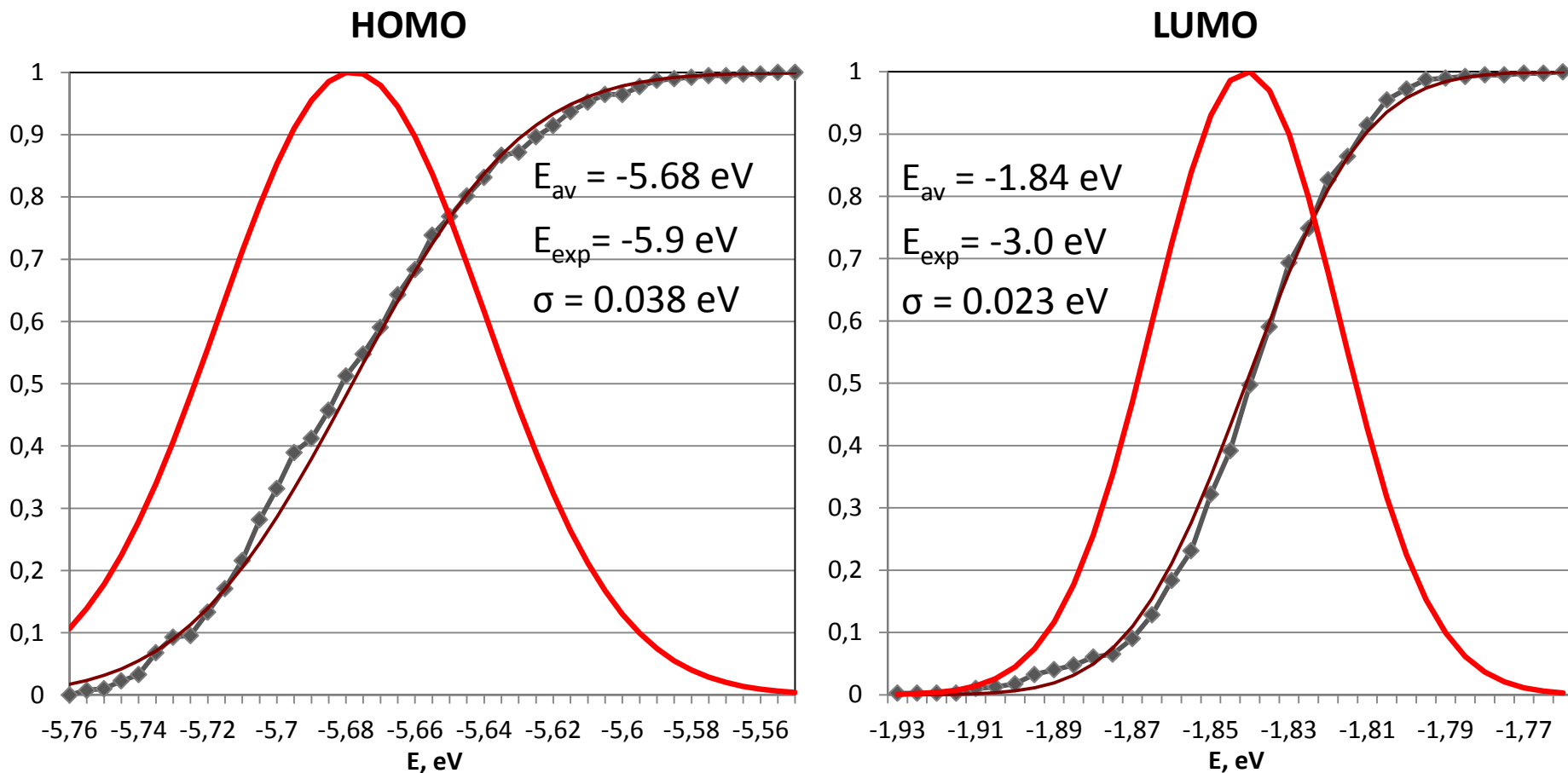


Modeling of the BA1q layer

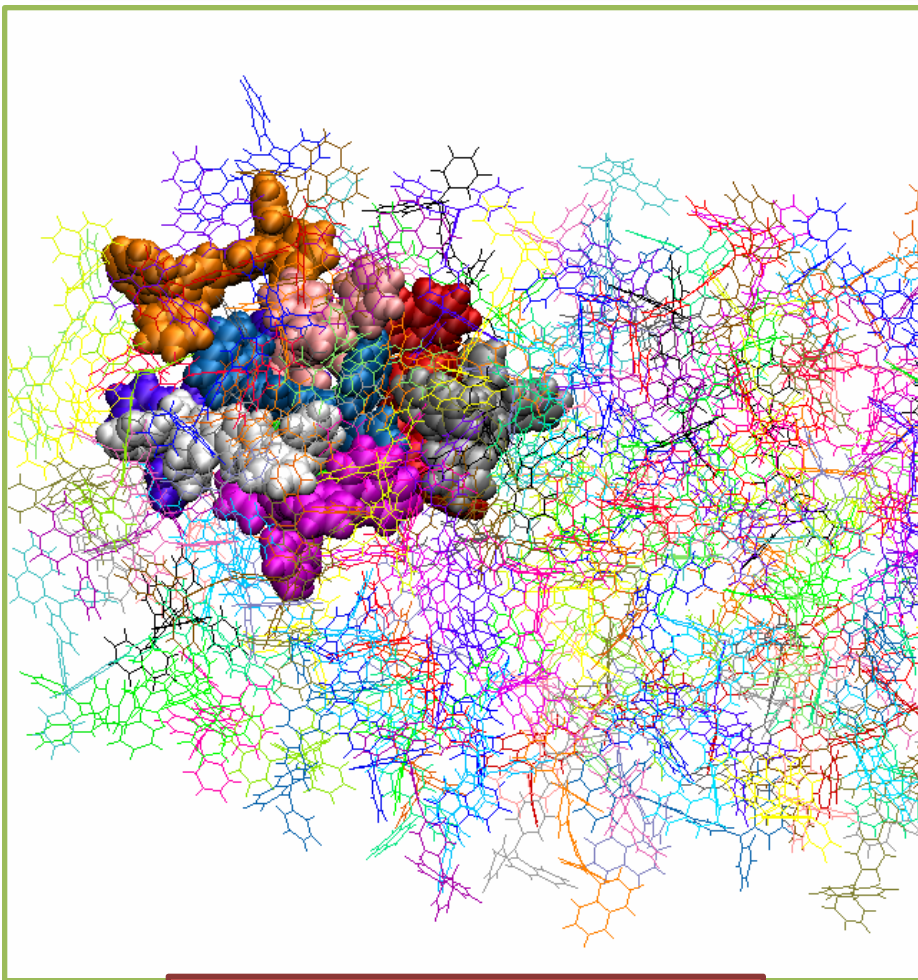


Distribution of Balq HOMO and LUMO energies (PCM)

method: DFT-D, PBE0, Basis set: 6-311(d,p), PCM: $R_{\text{SOLVENT}} = 8 \text{ \AA}$, $\epsilon = 3$, $\epsilon_{\text{inf}} = 3$, 300 molecules

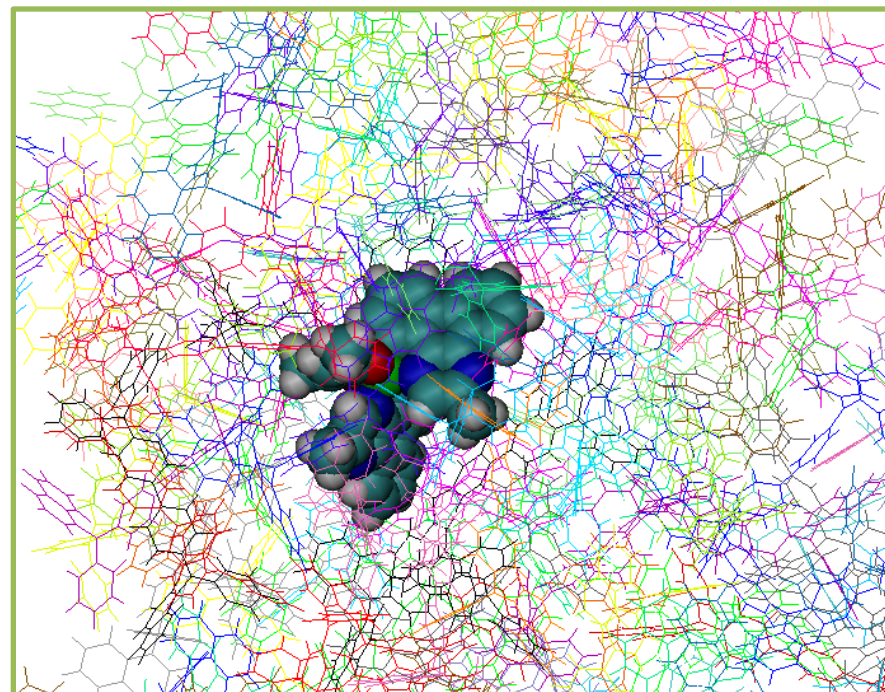


Microstructure of the recombination layer



Amorphous α -NPD layer

Periodic cell size: 9.58x 9.58 x 9.58 nm
1000 a-NPD molecules

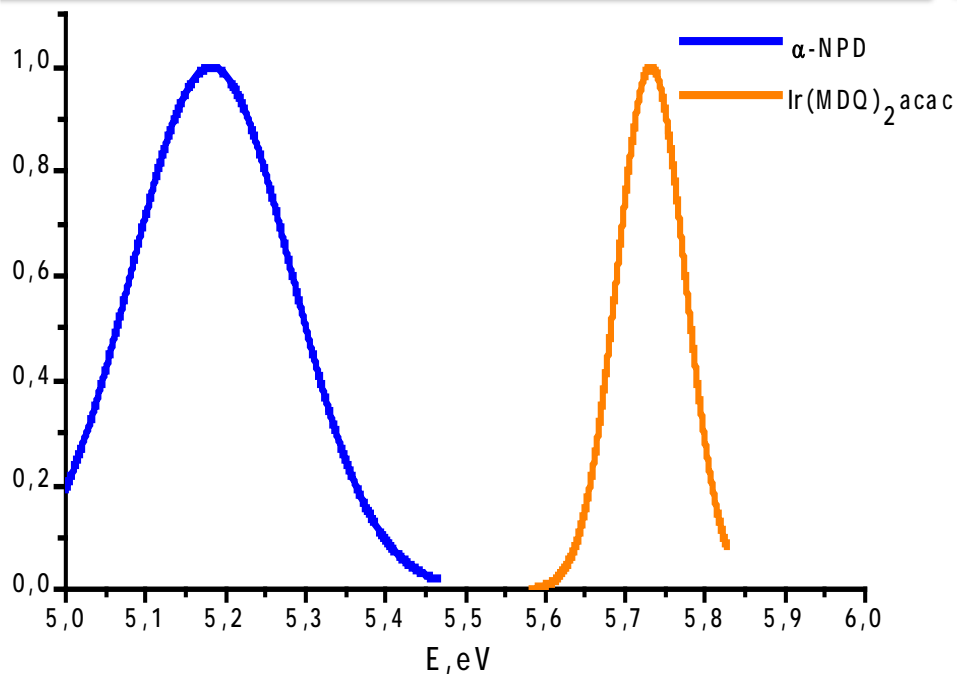


Ir(MDQ)₂acac in amorphous α -NPD layer

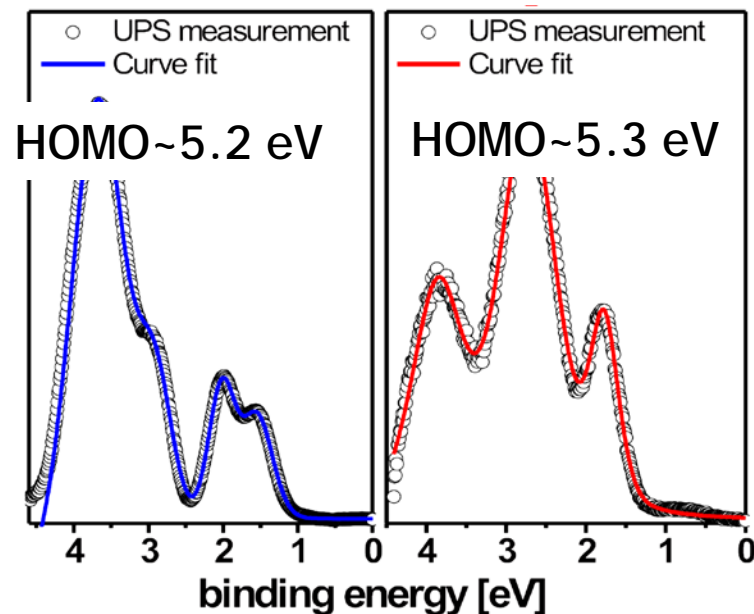
Periodic cell size: 4.7x 4.7 x 4.7 nm
122 a-NPD and 1 Ir(MDQ)₂acac molecules

Charge transport characteristics

Distribution of the IP energy of molecules in the recombination layer



UPS measurements for pure a-NPD (left) and Ir(MDQ)₂acac (right)

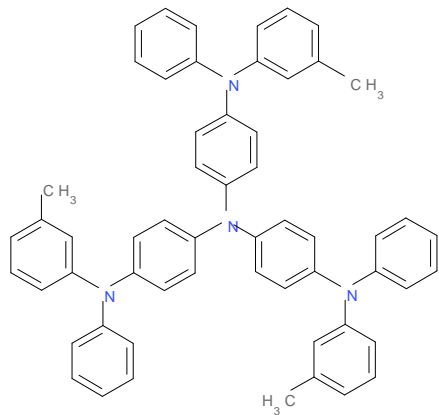


Binding energy = $E_{vac} - E_{Fermi}$; $E(Fermi) = 4.1$ eV
 Phys. Rev. B. 2009. V. 79. P. 245308

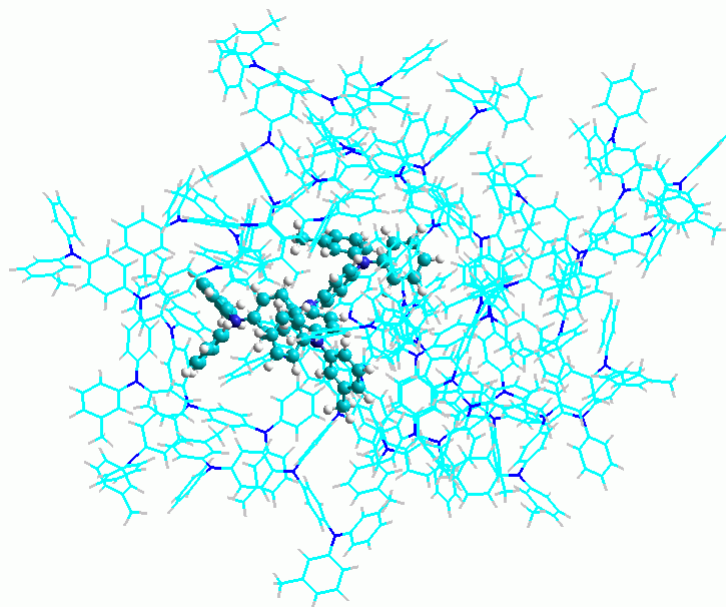
Charge transport characteristics for the layer:

Calculated	E(IP), eV	σ , eV	E(opt.gap), eV	E_{reorg} , eV
α -NPD	5.18 eV	0.1	3.13 eV	0.27 eV
Ir(MDQ) ₂ acac	5.73 eV	0.04	2.2 eV	

Modeling of the m-MTDATA layer

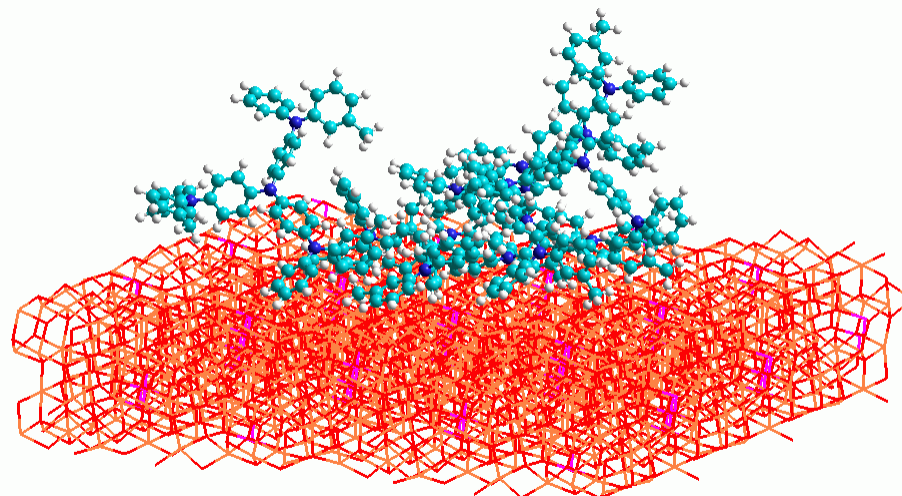
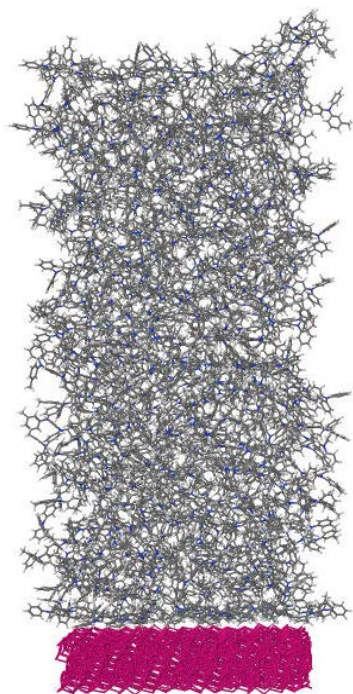


$I_{P}^{exp} = 5.0 \text{ eV}$



m-MTDATA molecule in its environment

m-MTDATA cell
on ITO surface



m-MTDATA molecules on ITO surface

Calculation PBE0/6-31G(d,p)

- Geometry optimized *in vacuo*

$$E(\text{HOMO}) = -4.520 \text{ eV}$$

$$\text{IP} = 5.38 \text{ eV}$$

$$\lambda = 0.416 \text{ eV}$$

- Geometry optimized in PCM ($\epsilon = 3$)

$$E(\text{HOMO}) = -4.528 \text{ eV}$$

$$\text{IP} = 4.74 \text{ eV}$$

$$\lambda = 0.332 \text{ eV}$$

- Average E(HOMO) and IP for a layer built by deposition of m-MTDATA molecules on ITO surface followed by MM optimization of the entire cell

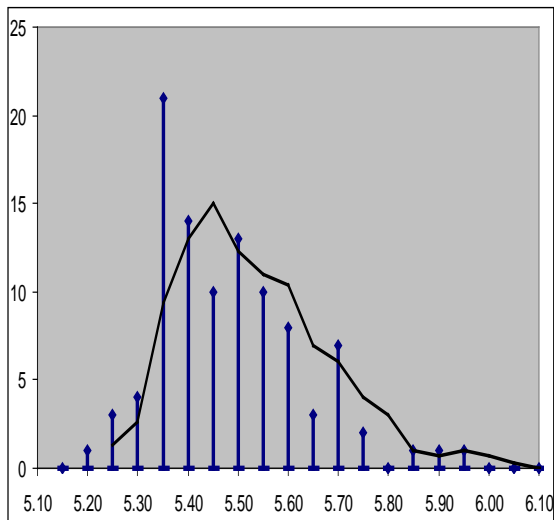
- Sample of 100 molecules

$$\text{IP}^{\text{av}} = 5.452 \text{ eV}, \sigma = 0.14 \text{ eV}$$

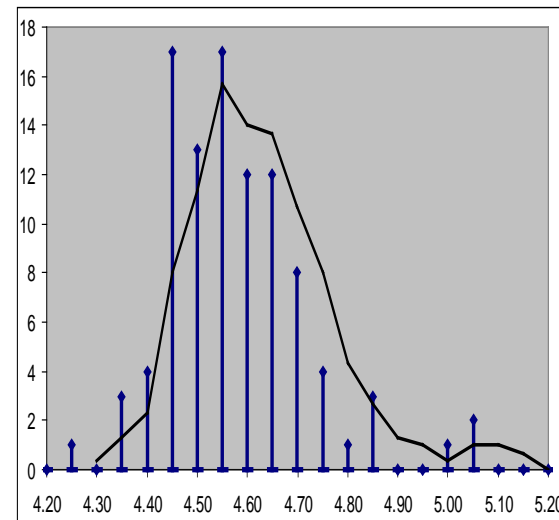
$$E(\text{HOMO})^{\text{av}} = -4.554 \text{ eV}, \sigma = 0.14 \text{ eV}$$

- Sample of 1000 molecules

$$E(\text{HOMO})^{\text{av}} = -4.559 \text{ eV}, \sigma = 0.15 \text{ eV}$$

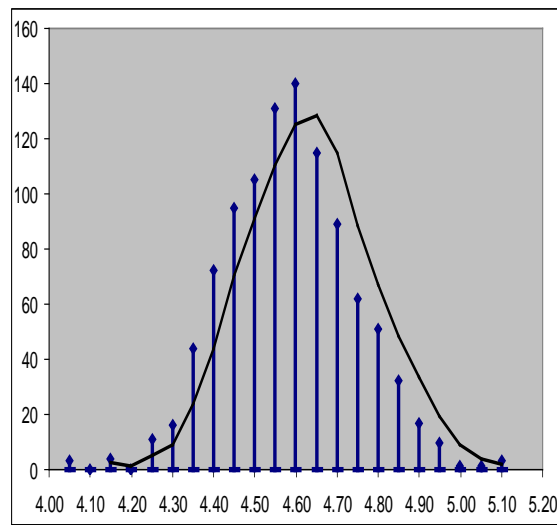


a



b

IP (a) and $-E(\text{HOMO})$ (b) in the sample of 100 m-MTDATA molecules

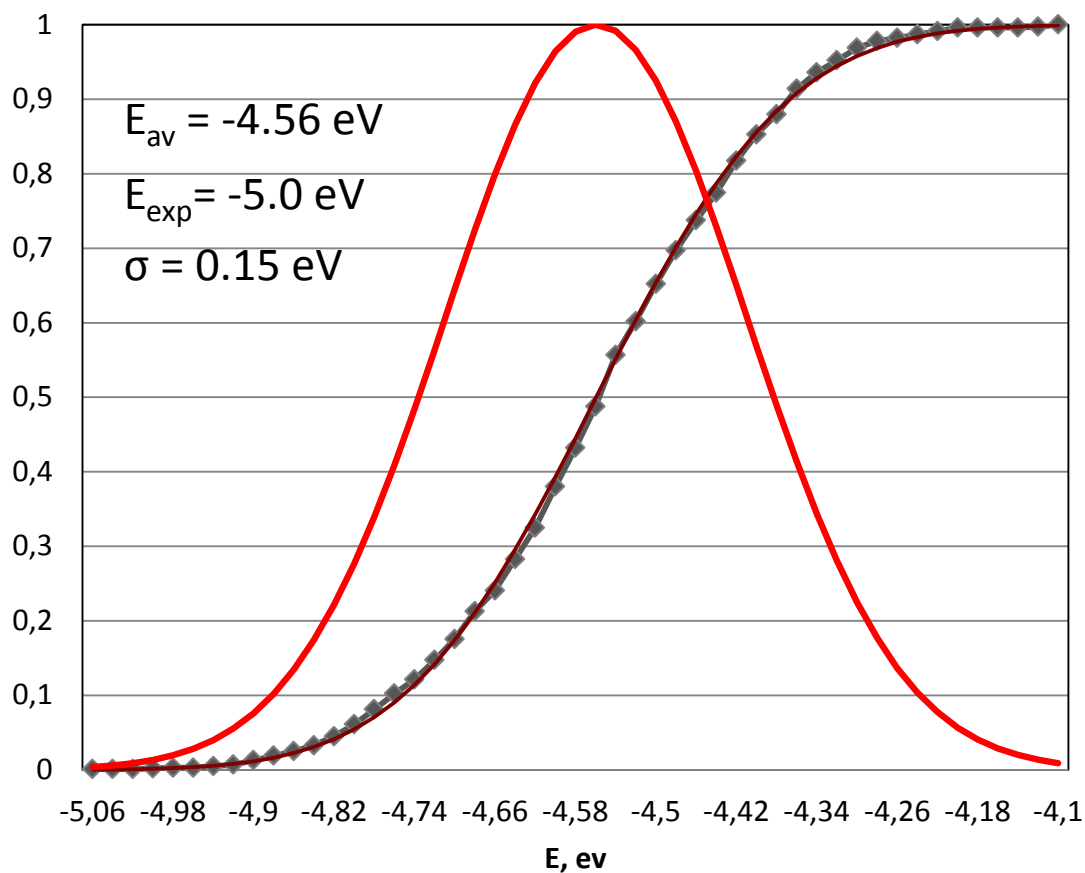


$-E(\text{HOMO})$ in the sample of 1000 m-MTDATA molecules

m-MTDATA Distribution of HOMO energies (PCM)

Method: DFT-D, PBE0, Basis set: 6-311(d,p),
PCM: $R_{\text{SOLVENT}} = 8 \text{ \AA}$, $\epsilon = 3$, $\epsilon_{\text{inf}} = 3$, 1000 molecules

HOMO



Final Conclusions

- ❑ **A methodology is developed for predictive atomistic multiscale simulations of the structure and functional properties of hierarchical organic and hybrid nanomaterials.**
- ❑ **The methodology is based on**
 - Atomistic quantum-chemical modeling of the structure and functional properties of the material at a molecular level.
 - Atomistic quantum-chemical (quantum-mechanical) modeling of the structure and properties of the material at a supramolecular level using MD and/or MC (kMC) methods and classical potentials (with parameters fitted using results of quantum-chemical calculations).
 - Quantum-chemical (quantum-mechanical) modeling of the absorption and emission spectra (or other required properties) for the system in a real environment (obtained from calculations at the supramolecular level) using DFT or even more accurate ab initio methods (CAS SCF, MCQDPT, etc.).
 - This approach is suitable for predictive modeling of materials for optical chemical sensors, microchips, OLEDs, quantum dots, quantum wells, and for other photonic applications.

This work has been made with the participation of

□ Our coworkers and coauthors from the laboratory of quantum chemistry and molecular simulation of the Photochemistry Center of Russian Academy of Sciences:

V. Chashchikhin, N. Dubinets, S. Emelyanova, A. Freidzon, K. Komarova, R. Minibaev, A. Odinokov, P. Rukin, and A. Safonov

□ Our colleagues and coauthors from other institutions

And due to permanent support from the director of Photochemistry Center Prof. M. Alfimov

□ Thank you very much for your attention!



Thank You !!!